Velocity, acceleration & jerk in electrospinning

A Menon, K Somasekharan

Citation

A Menon, K Somasekharan. *Velocity, acceleration & jerk in electrospinning*. The Internet Journal of Bioengineering. 2008 Volume 4 Number 2.

Abstract

Electrospinning can produce nano-fibers by drawing a polymer jet through a virtual spatio-temporal orifice. The diameter of the virtual orifice at any time or space depends on the velocity at that point, the velocity being determined by the continuity equation. Velocity profiles on silicone jet reveal that acceleration is not a constant, whereas the values fit the model for jerk. The findings should give a handle on the optimization of process parameters. To investigate the other factors that influence velocity (and hence the fiber diameter), the thinning and solidification are modeled. Results reveal that the jet thins drastically in the early stages, for both solution & melt electrospinning; however, thinning can continue till the end of the flight. In solution electrospinning, solvent evaporation during flight results in further thinning of the jet. The model reveals that solution electro-spun fibers deposited on the collector could be retaining some residual solvent, limiting its applications. The kinematic model for melt electrospinning computes velocity, fiber diameter, viscosity & temperature. The field gradient expressed in V/m is shown to be equivalent to N/C. In the range where the voltage matches the flow rate (and viscosity), a steady state is attained, resulting in continuous fibers. In this range, the process parameters of flow rate, viscosity or the voltage could be varied to give fibers of uniform diameter. The spool speed has to match the terminal velocity, for producing continuous fibers, to ensure dimensional stability of the product.

INTRODUCTION

Spinning is the process used for drawing a fiber-forming polymer into filaments by passing through a spinneret. Solution spinning (wet or dry) and melt spinning are the major spinning techniques used in the production of fibers. In dry spinning the solvent evaporates in a spinning tower, resulting in solid fibers; in melt spinning the polymer melt solidifies to give the fiber.

Conventional fiber-forming techniques are dependant on the spinneret diameter which may not be reduced indefinitely, due to limitations of the tools used for fabricating them. The major technique that can be used to make fibers thinner than 100 μm is electrospinning; the process is capable of giving very long continuous fibers [1-4].

Electrospinning produces very thin fibers by electrostatically drawing a polymer jet through a virtual spatio-temporal orifice. The diameter of the virtual orifice at any time or space depends on the velocity at that point. The velocity is determined at any point by the continuity equation: $Q = \pi r^2 v$, where Q is the volumetric flow rate, r is the fiber radius and v is the velocity.

END-OF-FLIGHT VELOCITY

Dalton et al., have melt electrospun poly-(ethylene glycol-block-ε-caprolactone) [5]; with scanning electron microscopy, they have determined the diameter of the fibers. Using their data and the continuity equation, we have computed the terminal velocities (Table 1). Whether the velocity is built up by constant acceleration or by jerk is investigated in this paper; the findings should give a handle on the optimization of process parameters.

Figure 1

Table 1. Computation of end-of-flight velocities, using continuity equation

Sample	Rate, mL / h	Diameter, nm	Velocity, m/s
Dalton-1	0.01	547.	24.
Dalton-2	0.01	211.	159.
Dalton-3	0.05	379.	123.
Dalton-4	0.05	1053.	8.
Dalton-5	0.10	1221.	24.
Dalton-6	0.10	1137.	27.
Dalton-7	2.00	337.	311.
Dalton-8	2.00	379.	246.

ELECTROSPINNING TECHNIQUE

Electrospinning technique employs very high electrostatic fields to draw polymers into very thin filaments. The spinneret is connected to one terminal of a high voltage supply; the electrostatically drawn polymer gets collected on the oppositely charged electrode, called a collector. Drastic reduction in diameter is achieved by this process and continuous fibers of nanometer diameters can be produced. These are usually collected as non-woven mats or as aligned fibers over a rotating mandrel.

The most common form of electrospinning is from polymer solutions, in a method similar to conventional dry spinning; the basic difference is that the limit imposed by the spinneret diameter is overcome by the electrostatic drawing potential. Electrospinning from melts, known as melt electrospinning, is also being practiced.

Electro-spinning assembly consists of the following: (1) high-voltage DC supply, (2) polymer reservoir & spinneret & (3) a metallic collector plate. The power supply provides ripple-free output, from a few to several tens of kilovolts. The reservoir-spinneret unit is connected to one of the terminals of the high-voltage supply. A screw-driven piston may be used to transport the polymer inside a syringe to a metallic needle. This mechanism has the advantage that the flow rate can be controlled and metered, based on the piston displacement. A metal foil may be placed over a metal plate, connected either to the opposite or earth terminal, to collect electro-spun fibers as non-woven mats. For collecting aligned fibers, a number of designs may be found in the literature [1] .

THE MECHANISM

The polymer jet is expected to have three regions during its trajectory to the collector [1] : (1) jet initiation, (2) jet thinning & (3) jet solidification.

Jet initiation process starts with a hemispherical charged droplet at the tip of the capillary. The droplet is under the influence of electrostatic attraction, which is balanced by surface tension [6] . Now, if the voltage is progressively raised, the droplet deforms and is pulled into a cone as described by Taylor. The Taylor cone designates the condition at which the two forces are balanced. The voltage at this condition is called the critical voltage [6] .

Beyond the critical voltage the electrostatic forces overcome the surface tension; the jet starts elongating and accelerating towards the collector. The increased velocity causes drastic thinning of the jet. In solution electrospinning, solvent evaporation during flight results in further thinning of the jet.

Jet solidification takes place due to cooling or due to solvent evaporation. A fiber now would have approached its final diameter. If any thinning takes place in this region, it is visco-elastic. The fibers are then collected on the collector plate. As will be discussed later, the solution electro-spun fibers deposited on the collector could be retaining some residual solvent. This solvent has to diffuse out through solid fibers over a period of time.

PROCESS VARIABLES

The important material characteristics that influence electrospinning are: (1) ionization potential/ electron affinity/ polarizability, (2) viscosity & (3) surface tension. The important process variables are (1) field characteristics & (2) flow rate.

The field characteristics are defined by (1) the polarity, (2) applied voltage & (3) electrode gap. The electrostatic field under which the polymer jet elongates and thins into nano-fibers is one of the most important and easily controllable process variables. The field gradient expressed in V/m is equivalent to N/C. (That is, a particular potential gradient expressed in volts per meter can be thought of as the force in newtons experienced by a unit charge of one coulomb in the jet.) This comes directly from Coulomb's law of electrostatic force of attraction.

$F = (1/4\pi\varepsilon) q_1 q_2 / r^2$ …(1.a)

or $F / q_2 = (1/4\pi\varepsilon_0) q_1 / r^2$ …(1.b)

Since $(1/4\pi\varepsilon_0) q_1/r = E$,

F / q_2 (in N/C) = E / r (in V/m) …(2)

where F is electrostatic force of attraction in N,

E is electrostatic potential in V,

q_1 and q_2 are two point charges, and

r is the distance of separation between the two charges.

Assuming that there is a point charge of 1 coulomb in the jet as the jet emerges from the spinneret, under the potential gradient it experiences a force which accelerates it to the opposite electrode. The creation of the charge in the jet would depend on the dielectric constant & electron affinity/ ionization potential of the solvent or the polymer.

Flow rate is another major process variable in electro-spinning. During spinning, it acts in tandem with viscosity. Unless the electrostatic force matches this combination of flow rate & viscosity, continuous fibers of uniform diameter cannot be expected. If the flow rate is too slow or if the voltage is too high, the initial droplet at the tip of the spinneret starts drawing; as the material is drawn faster than it is fed, eventually it gets detached. The drawing will resume after a new droplet is formed and the critical condition is attained. The non-steady state never transforms to the steady state.

If the flow rate is too fast, the droplet at the tip of the spinneret will grow in size and will drip from time to time; the steady state for spinning is not established. In the range where the voltage matches the flow rate (and viscosity), the initial non-steady state passes on to a steady state, resulting in continuous fibers. In this range, the process parameters of flow rate, viscosity or the voltage could be varied to give fibers of uniform diameter.

APPLICATIONS IN BIOMEDICAL NANOTECHNOLOGY

The surge in interest in electro-spinning in recent years was mainly driven by the nano-technology revolution. A nano-structure is defined as a structure with at least one dimension less than 100 nm. Melt electro-spinning is suggested for a number of applications [1-4] : (1) scaffolds for tissue engineering; (2) wound dressings & sutures; (3) cardio-vascular grafts; (4) controlled drug delivery systems in medicine & agriculture; (5) filtration of sub-micron particles in industrial separation; (6) reinforcement and solar sails; (7) non-wetting textile surfaces & protective clothing; (8) nano-tube construction & optical sensors etc.

An interesting direct in vitro electro-spinning was reported by Dalton et al. [7] Here, melt electro-spun fibers were collected directly over cell lines. Poly(ethylene glycol-b-caprolactone), blended with poly(caprolactone), was spun over fibroblast cell lines. In six days, the cells had established on the polymer scaffold; their morphology had changed from flat to spindle shaped. This indicates the possibility of layer-on-layer tissue constructs.

Melt electro-spinning could have certain advantages over solution electrospinning [2-4] : (1) melt electro-spinning can be looked at as a pure fluid-dynamics problem; solvent evaporation complicates solution electro-spinning; (2) jet branching & multi-jet formation are not observed in melt electro-spinning; (3) jet whipping of solution electro-spinning is not conspicuous here; (4) rate of spinning & yield are higher; (5) problems related to solvent removal can be avoided; (6) possibility of better blended polymer fibers; (7) possibility of direct in vitro (over cell lines) & direct in vivo (wound dressing) spinning. The disadvantages to be overcome in process design are: (1) fiber diameters are an order of magnitude larger than solution electro-spun fibers; (2) viscosities of melts are higher; (3) operating temperatures are higher; (4) applied potentials are higher.

MODELING

For optimization of process parameters, one has to investigate whether the velocity is built up by constant acceleration or by jerk; other factors that might influence velocity (and hence the fiber diameter) have to be unraveled as well. The spool speed also has to match the terminal velocity, for producing continuous fibers (for example, to make vascular grafts), to ensure dimensional stability of the product. For this, the thinning and solidification (solvent evaporation in solution spinning and cooling in melt spinning) are modeled first. The information is also required for direct in vitro & direct in vivo biomedical applications.

NUMERICAL ANALYSIS FOR SOLUTION ELECTROSPINNING

A numerical analysis was carried out to compute solvent evaporation and fiber thinning. The spinning conditions were:

Applied Potential = 10 kV

Electrode Gap = 10 cm

Spinneret Diameter = 1.19 mm

Flow Rate = 0.012 mL / minute

Assumptions of the model:

(1) Single jet thins as it traverses towards the collector;

(2) Solvent loss by radial diffusional mass transfer;

(3) Diffusivity of solvent decreases as concentration increases;

(4) Uniform velocity, as the charge carriers are lost during the flight.

Parameters:

Self-diffusion coefficient of chloroform = 1.0 x 10^{-9} m^2 s^{-1}

Diffusivity of chloroform in PCL = 1.0 x 10^{-13} m^2 s^{-1}

Time of flight (from final fiber diameter) = 7.52 ms

Grid length = 1 mm.

The results of this calculation are given in Table 2. It can be seen that about 27% of the solvent is retained at the time of deposition. This means that the spun mat has to go through a drying stage; this is especially the case with carcinogenic solvents and for very sensitive mammalian cell lines. Hence, solution electro-spinning is not suited for direct in vitro or direct in vivo applications.

Figure 2

Table 2. Drying and thinning of the jet during solution electrospinning

Grid no.	Solvent Remaining, %	Diffusivity x 10^{10}, m^2 s^{-1}	Fiber Diameter, nm
2	90.2	4.09	688
3	88.9	4.04	683
4	87.6	3.99	679
5	86.4	3.94	674
6	85.1	3.90	670
7	83.9	3.85	666
8	82.7	3.80	661
9	81.5	3.75	657
10	80.3	3.70	653
20	69.5	3.23	612
40	52.4	2.37	542
60	40.5	1.68	487
80	32.3	1.19	446
100	26.6	0.853	415

MODEL FOR MELT ELECTROSPINNING

For solution electrospinning, it is reasonable to assume that the jet is charged throughout. However, a uniform charging is not a valid assumption for melt electrospinning. In this case, the viscosity is higher and a laminar flow is more valid. Charging of polymer melt would take place only at the interface. In the applied electrostatic field, only the charged skin would experience the drawing force. However, it will be transmitted to the layers beneath by viscous forces between the layers.

VISCOSITY VARIATION WITH TEMPERATURE

For a flow model, as stated above, the variation of viscosity with temperature is important. At high temperatures and low viscosities, electrospinning is governed by viscous flow; as temperature decreases, viscosity increases and the deformation becomes visco-elastic. So the jet could have two regimes – a viscous flow & visco-elastic drawing.

The characterization of the variation of viscosity with temperature is required to ascertain where one regime transforms to the other. Ideally a cone-and-plate viscometer is used to characterize the variation of viscosity with temperature. Here the hole theory of viscosity [8] is used to calculate the variation of viscosity with temperature. As per the theory, each fluid element will have an associated free volume. The activation energy to move the actual mass into this free volume during flow gives rise to viscosity.

$\eta = A \exp(\Delta G^* / RT)$ …(3)

The viscosities reported by Dalton et al. [5] were curve fitted to estimate the activation energy and pre-exponential factor (Table 3). The values reported are over a wide range of molecular weights (Mn = 8,000 – 31,000) and over a range of temperature (60°C - 90°C). The correlation coefficients for the log vs. 1/T regression analysis is excellent in all cases; and the computed activation energies are in amazing agreement. Hence these values were used in the present studies, to estimate the viscosities at various temperatures.

Figure 3

Table 3. Least squares regression analysis, of the viscosity values of Dalton et al., for log η vs. 1/T

Parameters	PEG_{47}-b-PCL_{55}	PEG_{47}-b-PCL_{95}	PEG_{47}-b-PCL_{120}	PEG_{119}-b-PCL_{189}	PEG_{119}-b-PCL_{240}
Mn	7,689	12,255	15,108	25,146	31,309
Slope	3,838.6	3,472.5	3,560.8	3,634.0	3,702.1
Intercept	-10.74	-8.167	-7.620	-6.690	-6.661
R_{sq}	0.989	0.999	0.998	0.998	0.999
E_a (kJ/mol)	31.9	28.9	29.6	30.2	30.8

Hagen-Poiseuille equation was used for estimating the melt viscosity for PCL-42500 at all temperatures of interest (60-200°C); for computing the variation of viscosity with temperature, the melt flow index at 80°C (quoted by the manufacturer), along with the computed activation energy & pre-exponential factor was used.

Melt Viscosity () = ($\pi r^4 \Delta p$) / (8 Q L) …(4)

where (as per ASTM D123873),

r = radius of the capillary, 0.5725 mm;

L = length of the capillary, 8.0 mm;

Δp = pressure drop, 0.3 MPa;

Q = volumetric flow rate;

Q = (MI) / (60.0),

where MI = 1.90 g per 10 minutes & = 1.32 g per cm^3.

The results are given in Table 4.

Figure 4

Table 4. Melt viscosity variation of PCL-42500 with temperature (predicted as detailed in the test)

Temperature (°C)	Viscosity (Pa s)
60	927.7
80	499.2
100	287.1
120	174.7
140	111.5
160	74.2
180	51.2
200	36.4

KINEMATIC MODEL

The numerical analysis of a kinematic model was programmed in C/C++. In this model, volume of polymer being transported across control surfaces of finite element grids along the electrospinning axis is monitored. The following assumptions are made for modeling.

(1) Only a single jet is being electro-spun.

(2) Steady state has been achieved.

(3) Each of the finite elements experiences a constant acceleration during its flight to the collector.

The model computes velocities & fiber diameters at the ends of each finite element, using continuity. Temperature profile is calculated using a lumped capacitance approximation.

LUMPED CAPACITANCE APPROXIMATION

Lumped capacitance model is a treatment for transient conduction problems. It is used to calculate cooling with time for bodies suddenly exposed to changes in environmental temperatures. This model assumes a uniform spatial distribution within the body and convection conditions at the interface. An energy balance at the surface is as follows: Rate of heat loss at the surface = Rate of change of internal energy.

$- h A_s (T - T_\infty) = m c_p (dT / d)$ …(5.a)

$- (h A_s / m c_p) d = dT / (T - T_\infty)$ …(5.b)

Integrating,

$- (h A_s / m c_p) \theta + C = \ln (T - T_\infty)$ …(6)

At $\theta = 0$, $C = \ln (T - T_\infty)$

Substituting

$- (h A_s / m c_p) \theta = \ln [(T - T_\infty) / (T - T_\infty)]$ …(7.a)

$(T - T_\infty) / (T - T_\infty) = \exp (- (h A_s / m c_p) \theta)$ …(7.b)

where h = convective heat-transfer coefficient;

A_s = surface area of the control volume;

m = mass of the control volume;

c_p = specific heat;

T = initial temperature;

T_∞ = sink temperature;

T = temperature of the control volume after time θ.

This model assumes a Newtonian cooling; hence the model is valid only when the non-dimensional number called Biot number,

$Bi = (h s / k) < 0.1$,

where k = thermal conductivity and

s = characteristic length (radius of the fiber, in this case).

The estimated Biot number in the present study is of the order of 0.001, satisfying the condition.

For cooling of the jet, radial heat conduction by Fourier's law was attempted. As the convergence criteria [11] could not be met for the system with very low Biot number, realistic results were not obtained – lumped capacitance is the method of choice.

THE PROGRAM

The inputs to the program are (1) feed rate to the spinneret, (2) the electrode gap and (3) the final fiber diameter. The program returns (1) the variation of velocity, (2) the fiber diameter & (3) the temperature profile along the spinning axis. The program was operated with the melt electro-spinning parameters of Dalton et al. [5] :

Flow rate = 0.02 mL per hour;

Final diameter of the fiber = 211 nm;

Electrode gap = 30 cm.

For calculating temperature profile,

Initial temperature = 200°C;

Ambient temperature = 30°C;

Convection heat-transfer coefficient, h = 75 w $m^{-2} K^{-1}$;

Thermal conductivity = 0.204 w $m^{-1} K^{-1}$;

Specific heat, c_p = 1507 J $kg^{-1} K^{-1}$.

ALGORITHM

Inputs: Flow rate, final fiber diameter & electrode gap.

Step 1: Compute velocities at spinneret exit and at collector, using Q = AV.

Step 2: Calculate acceleration using V2 - U2 = 2aS.

Step 3: Compute velocity profile along fiber axis for 1mm grids, using V2 - U2 = 2aS.

Step 4: Compute fiber diameter, along fiber axis, for 1mm grids, using Q = AV.

Step 5: Compute temperature variation along fiber axis using a lumped capacitance model.

DISCUSSION

The model suggests that major reduction in diameter takes place within 5 cm from the spinneret (Table 5). By this time, temperature would have dropped to such an extent that the PCL-42500 would have built up viscosity above 200 Pa s. Hence there may be two regions in the flow – a purely viscous and a visco-elastic. The viscous region may extend up to 5 cm from the spinneret and hence this is where the largest reduction takes place. If further reduction in fiber diameter is required:

(1) The temperature of the heated zone may be increased by 10-20°C (the polymer will not start decomposing below 225°C in air);

(2) The molecular weight of the polymer may be reduced from 42,500, which will lower its viscosity (the mechanical properties will not decrease appreciably, till the molecular weight falls below 24,000);

(3) The applied potential may be increased beyond the 20 kV used (no spraying is expected for this polymer at voltages below 30 kV);

(4) Auxiliary heating beyond the spinneret will increase the

region of high deformation, leading to decrease in fiber diameter;

(5) Lowering the feed rate also will decrease the fiber diameter. The model suggests that the five parameters can be optimized.

Figure 5

Table 5. Predictions of the kinematic model for melt electrospinning

Grid Number	Temperature, °C	Viscosity, Pa s	Velocity, m / s	Fiber dia, nm
1	200	36	0.0000049	1200000
2	194	40	9.2	878
3	191	42	13.0	738
4	188	44	15.9	667
5	186	46	18.3	621
6	184	48	20.5	587
7	182	49	22.5	561
8	180	51	24.3	540
9	179	53	25.9	522
10	177	54	27.5	507
50	135	124	64.2	332
100	106	245	91.3	278
200	74	590	129.4	234
301	58	1004	158.9	211

EXPERIMENTAL VERIFICATION OF ACCELERATION VS. JERK

As the models suggest that drawing can take place till the end of the flight, the task is to experimentally verify whether the velocity is determined by acceleration or jerk.

With a model fluid (Dow-Corning 200 silicone oil), Larrondo & Manley have measured [12] the point velocities in various regions of the flow field, using cine photography. We have read out the data from their diagrams, after making the required program in the professional standard authoring tool, Macromedia Flash MX; the readings are given in Tables 6.A-6.D.

Figure 6

Table 6A. Velocity profile along flight axis, at 6 kV cm^{-1} & at radial distance 0.10 cm (extracted from Larrondo & Manley)

	Axial Distance, cm	Velocity, cm s^{-1}
1	0.321	0.0590
2	0.305	0.0553
3	0.293	0.0486
4	0.280	0.0456
5	0.261	0.0407
6	0.241	0.0382
7	0.221	0.0336
8	0.202	0.0293
9	0.181	0.0248
10	0.161	0.0223
11	0.139	0.0192
12	0.132	0.0162
13	0.121	0.0153

Figure 7

Table 6B. Velocity profile along flight axis, at 7 kV cm^{-1} & at radial distance 0.10 cm (extracted from Larrondo & Manley)

	Axial Distance, cm	Velocity, cm s^{-1}
1	0.323	0.0750
2	0.300	0.0677
3	0.285	0.0636
4	0.260	0.0575
5	0.232	0.0476
6	0.219	0.0441
7	0.198	0.0407
8	0.172	0.0343
9	0.149	0.0279
10	0.137	0.0250
11	0.127	0.0238
12	0.120	0.0218

Figure 8

Table 6C. Velocity profile along flight axis,
at 6 kV cm^{-1} & at radial distance 0.03 cm (extracted from Larrondo & Manley)

	Axial Distance, cm	Velocity, cm s^{-1}
1	0.320	0.0982
2	0.299	0.0895
3	0.291	0.0831
4	0.278	0.0784
5	0.260	0.0674
6	0.240	0.0593
7	0.221	0.0511
8	0.199	0.0453
9	0.182	0.0407
10	0.172	0.0369
11	0.159	0.0343
12	0.140	0.0296
13	0.122	0.0255

Figure 9

Table 6D. Velocity profile along flight axis,
at 7 kV cm^{-1} & at radial distance 0.03 cm (extracted from Larrondo & Manley)

	Axial, Distance, cm	Velocity, cm s^{-1}
1	0.300	0.113
2	0.285	0.0991
3	0.260	0.0851
4	0.240	0.0758
5	0.220	0.0683
6	0.199	0.0575
7	0.183	0.0523
8	0.174	0.0488
9	0.162	0.0462
10	0.152	0.0421
11	0.149	0.0383
12	0.136	0.0363
13	0.122	0.0302

Since $V^2 - U^2 = 2aS$, and since V >>> U, if acceleration is constant, a plot of V^2 vs. S (axial distance) should be linear. Least-squares regression analysis should give the slope as 2a and intercept as zero. Using correlation coefficient as the criterion for the goodness of fit, we find that acceleration is not a constant (Table 7); this is corroborated on plotting the graph (Figure 1).

To verify the presence of jerk, the Newton's Law, F = ma, may be combined with Coulomb's Law, $F = (q_1 q_2 / 4 \pi \varepsilon) (1 / r^2)$:

$a = (A / m) (1 / r^2)$ …(8.a)

where $A = (q_1 q_2 / 4 \pi \varepsilon)$.

Or $a = B / r^2$ …(8.b)

where $B = (q_1 q_2 / 4 \pi \varepsilon m)$

Since $V^2 - U^2 = 2aS$, and since V >>> U,

$V^2 = 2aS$. …(9.a)

Substituting the value of acceleration (a)

$V^2 = 2 (B / r^2) S$ …(9.b)

Since r = (S – S), where S is the constant electrode gap,

$V = C^{0.5} S^{0.5} / (S - S)$. …(10)

The plot of V versus $S^{0.5} / (S - S)$ should be linear, with zero intercept, the slope being the square root of $(q_1 q_2 / 2 \pi \varepsilon m)$. Least squares regression analysis reveals that the fits are good (Table 7); this is corroborated by plotting the graph (Figure 2). The jerk model is validated.

Figure 10

Table 7. Deciding between constant acceleration (1) and jerk (2),
for data sets 6A-6D

Data & Fit	Slope	Standard Deviation	Intercept	Correlation Coefficient
A-1	0.015	0.001	-0.002	0.956
A-2	0.277	0.013	-0.038	0.988
B-1	0.024	0.001	-0.003	0.978
B-2	0.342	0.009	-0.043	0.997
C-1	0.044	0.004	-0.006	0.957
C-2	0.491	0.025	-0.072	0.986
D-1	0.060	0.005	-0.008	0.960
D-2	0.577	0.026	-0.081	0.989

Figure 11

Figure 1 – Model for constant acceleration (does not fit experimental points)

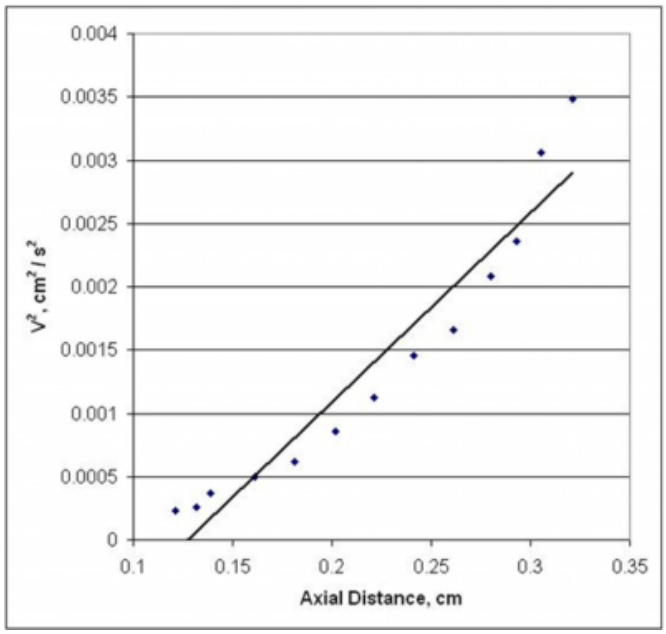

Figure 12

Figure 2 – Model for jerk (does fit experimental points)

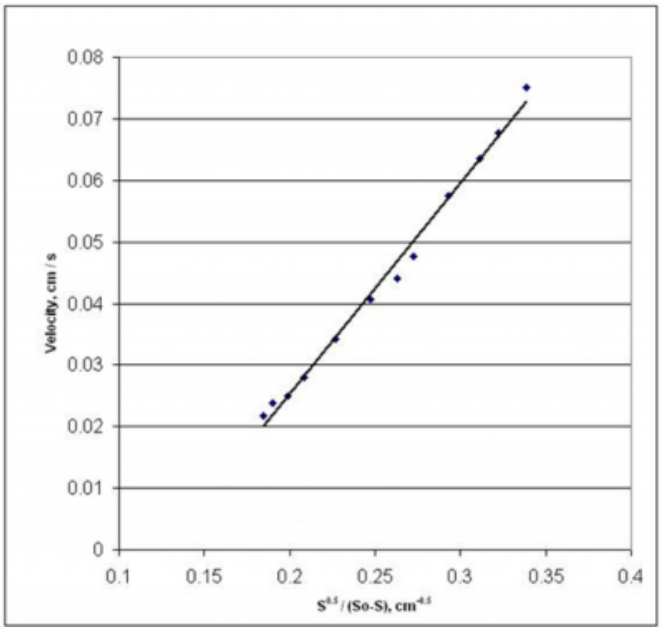

CONCLUSIONS

The surge in interest in electrospinning in recent years is mainly driven by the nano-technology revolution. Electrospinning, the major technique capable of making very long continuous nano-fibers, is suggested for a number of biomedical applications like scaffolds for tissue engineering, cardio-vascular grafts, etc.

Electrospinning produces very thin fibers by electrostatically drawing a polymer jet through a virtual spatio-temporal orifice. The diameter of the virtual orifice at any time or space depends on the velocity at that point. It is shown that the velocity is determined at any point by the continuity equation.

Whether the velocity is built up by constant acceleration or by jerk is investigated in this paper. Experimental values [12] of velocity profiles on silicone jet reveal that acceleration is not a constant; the experimental values fit the model for jerk. The findings should give a handle on the optimization of process parameters. Other factors that influence velocity (and hence the fiber diameter) have also been analyzed.

For this, the thinning and solidification (solvent evaporation in solution spinning and cooling in melt spinning) are modeled. Results reveal that the increased velocity causes drastic thinning of the jet in the early stages, for both solution & melt electrospinning. The models also reveal that thinning can continue till the end of the flight, determined by the continuity equation. It should be possible to produce continuous fibers of nanometer diameters by both processes.

In solution electrospinning, solvent evaporation by radial diffusional mass transfer during flight results in further thinning of the jet. The model reveals that solution electro-spun fibers deposited on the collector could be retaining some residual solvent. Hence, solution electro-spinning may not be suitable for direct in vitro or direct in vivo applications.

In the kinematic model for melt electrospinning, the volume of polymer being transported across control surfaces of finite element grids along the spinning axis is monitored. The model computes velocities & fiber diameters at the ends of each finite element, using continuity. Temperature profile is calculated using a lumped capacitance approximation; since the Biot number in the present study is of the order of 0.001, the model is valid. The variation in viscosity during flight is estimated by = A exp (G* / RT).

The electrostatic field under which the polymer jet elongates and thins into nano-fibers is one of the most important and easily controllable process variables. The field gradient expressed in V/m is shown to be equivalent to N/C, the force experienced by a unit charge in the jet.

Flow rate is another major process variable in electro-spinning. During spinning, it acts in tandem with viscosity. In the range where the voltage matches the flow rate (and

viscosity), the initial non-steady state passes on to a steady state, resulting in continuous fibers. In this range, the process parameters of flow rate, viscosity or the voltage could be varied to give fibers of uniform diameter.

The spool speed has to match the terminal velocity, for producing continuous fibers (for example, to make vascular grafts), to ensure dimensional stability of the product.

References

1. Huang Z-M, Zhang Y-Z, Kotaki M & Ramakrishna S, A review on polymer nano-fibers by electro-spinning and their applications in nano-composites, Compos Sci Technol, 63 (2003) 2223-2253.
2. Rangkupan R & Reneker D H, Electrospinning process of molten polypropylene in vacuum, Journal of Metals, Materials & Minerals, 12 (2003) 81-87.
3. Lyons J, Li C & Ko F, Melt electro-spinning, Part I: processing parameters and geometric properties, Polym, 45 (2004) 7597-7604.
4. Lyons J M, Melt electro-spinning of thermoplastic polymers: an experimental & theoretical analysis, Ph D Thesis, Drexel University, Philadelphia, USA, 2004.
5. Dalton P D, Calvet J L, Mourran A, Klee D & Möller M, Melt electrospinning of poly(ethylene glycol-b-caprolactone), Biotechnol J, 1 (2006) 998-1006.
6. Taylor G I, Electrically driven jets, Proc R Soc London, Ser A, 313 (1969) 453-475.
7. Dalton P D, Klinkhammer K, Salber J, Klee D & Möller M, Direct in vitro electrospinning with polymer melts, Biomacromolecules, 7 (2006) 686-690.
8. Glasstone S, A Textbook of Physical Chemistry, (MacMillan India Ltd, New Delhi) 1976.
9. White F M, Fluid Mechanics, 6th edn (Tata McGraw-Hill Publishing Company, New Delhi) 2008.
10. Incropera F P & DeWitt D P, Fundamentals of Heat & Mass Transfer, 5th edn (John Wiley & Sons, New Delhi) 2002, Chapter 5.
11. Crank J, The Mathematics of Diffusion, 2nd edn (Clarendon Press, Oxford) 1976.
12. Larrondo L & Manley R S, Electrostatic fiber spinning from polymer melts. II. Examination of the flow field in an electrically driven jet, J Polym Sci, Part B: Polym Phys, 19 (1981) 921-932.

Author Information

Arun Menon
School of Chemical- & Biotechnology SASTRA University, Thanjavur

KN Somasekharan
School of Chemical- & Biotechnology SASTRA University, Thanjavur